Communications on Applied Nonlinear Analysis
ISSN: 1074-133X
Vol 31 No. 1 (2024)

Analyse the Behaviour of Magnetic Fluid based Transversely Rough Long Bearing

Dr. Mital Patel[1], Dr. Niketa J. Savaliya[2], Dr. Mohit Diwan[3]

[1]Assistant Professor, Ahmedabad Institute of Technology, Ahmedabad, Gujarat, India
[2]Assistant Professor, P. P. Savani University, Surat, Gujarat, India
[3]Professor and HOD, Ahmedabad Institute of Technology, Ahmedabad, Gujarat, India
mital.kachhadia6611@gmail.com[1], nsavaliya24@gmail.com[2], diwanmohit@gmail.com[3]

Article History:
Received: 04-01-2024
Revised: 23-02-2024
Accepted: 26-03-2024

Abstract:
This study presents an investigation into the performance of a rough hydrodynamic slider bearing lubricated with a magnetic fluid. The applied magnetic field is considered oblique to the stator, and the bearing surfaces are assumed to exhibit transverse surface roughness characterized by a random variable with non-zero mean, variance, and skewness. Using stochastic averaging, the corresponding Reynolds equation is formulated and solved with appropriate boundary conditions to determine the pressure distribution, which is subsequently used to compute the load-carrying capacity. Numerical integration is performed using Simpson's 1/3 rule, and the results are illustrated graphically. The analysis indicates that transverse surface roughness adversely influences the performance of the bearing system. However, it is observed that in the case of negatively skewed roughness, the adverse effects can be partially mitigated due to the positive contribution of the magnetic field. The findings emphasize the importance of accounting for surface roughness during the design of magnetic-fluid-based slider bearings to achieve improved operational efficiency.
Keywords- Long bearing, Surface roughness, Magnetic fluid, Reynolds equation, Pressure, Load carrying capacity.

1. Introduction

The slider bearing is one of the most commonly encountered hydrodynamic bearings, primarily because its film-thickness expression is relatively simple and the boundary conditions—requiring zero pressure at the bearing ends—are straightforward. A key feature of any hydrodynamic slider bearing is the formation of a converging lubricant wedge, which enables pressure generation within the film. This converging wedge can be produced in several geometric configurations. Purdey (1947) established that the specific wedge shape is less important than the aspect ratio in achieving effective hydrodynamic action.

In slider bearings, the lubricant film is continuous and non-divergent, thereby eliminating the possibility of negative pressures. These bearings are typically designed to support axial loads. The classical analysis of hydrodynamic lubrication for non-porous slider bearings is well documented, with foundational treatments provided by Pinkus and Sternlicht (1961). The infinitely long slider bearing is, in fact, an idealized representation of a single sector-shaped pad in a hydrodynamic thrust bearing system. Such systems generally consist of a fixed or pivoting pad and a moving surface, which may be plane, stepped, curved, or of composite geometry. Due to their wide application in

clutch plates, automotive transmissions, and domestic appliances, squeeze-film slider bearings have been extensively studied (Prakash and Vij, 1973; Bhat and Patel, 1981). Various film shapes of slider bearings have also been analyzed (Pinkus and Sternlicht, 1961; Bagci and Singh, 1983; Hamrock, 1994), particularly in the context of supporting transverse loads.

It is well known that, after periods of operation and wear, bearing surfaces develop surface roughness. Contamination or chemical degradation of the lubricant can further contribute to this roughness. The roughness observed on bearing surfaces is generally random in nature and does not follow any deterministic structural pattern. This randomness was recognized in numerous early investigations (Mitchell, 1950; Davis, 1963; Burton, 1963; Tzeng and Saibel, 1967; Christensen and Tonder, 1969a, 1969b, 1970; Tonder, 1972; Berthe and Godet, 1973). Christensen and Tonder (1969a, 1969b, 1970) developed a comprehensive analytical framework for modeling the effect of transverse surface roughness using a general probability density function, extending the earlier work of Tzeng and Saibel (1967). Their method has since been widely applied to assess the influence of surface roughness (Ting, 1975; Prakash and Tiwari, 1982, 1983; Prajapati, 1991, 1992; Guha, 1993; Gupta and Deheri, 1996; Andharia, Gupta and Deheri, 1997, 1999).

All these studies were carried out using conventional lubricants. Magnetic fluids, however, present distinct advantages. These fluids are prepared by suspending ultra-fine magnetic particles—coated with a surfactant—in a magnetically passive carrier liquid such as hydrocarbons, benzene, or fluorocarbons. A unique characteristic of magnetic fluids is that they remain in a liquid state under the influence of a magnetic field and regain their original properties once the field is removed. When subjected to a magnetic field gradient, the suspended particles experience a force, inducing motion and drag within the fluid. One significant advantage of magnetic fluid lubrication is that the lubricant can be retained at a desired location using an external magnetic field (Bhat, 2003).

Several studies have investigated the role of magnetic fluids in bearing lubrication. Verma (1986) and Agrawal (1986) analyzed squeeze-film performance using magnetic fluid lubricants. Bhat and Deheri (1991) extended these analyses to examine squeeze-film behavior between porous annular disks under an oblique magnetic field, concluding that magnetic fluid lubrication significantly enhances bearing performance. Further, Bhat and Deheri (1991) analyzed a magnetic fluid-based porous composite slider bearing with a composite slider (inclined and flat pads), noting that magnetic fluid lubrication reduces friction and shifts the center of pressure toward the inlet while markedly increasing load-carrying capacity. In another investigation, Bhat and Deheri (1995) compared various geometric configurations of porous slider bearings, reporting that magnetic fluid lubrication generally increases load-carrying capacity and shifts the pressure center toward the outlet. Shah and Bhat (2003) developed a mathematical model to study the effect of slip velocity on a porous secant-shaped slider bearing lubricated with a ferrofluid using the Jenkins model. Deheri, Andharia, and Patel (2005) examined the performance of a transversely rough slider bearing with a magnetic-fluid-based squeeze film, demonstrating that appropriate magnetization parameters lead to significant performance enhancement. Their study also considered a magnetic fluid-based hyperbolic slider bearing and observed noticeable improvements in load-carrying capacity.

In this context, the present work proposes to analyze the performance of a magnetic-fluid-lubricated rough hyperbolic slider bearing.

2. Analysis:

The geometry and configuration of bearing system is shown in Figure 1, which is infinite in Z-direction, where in the slider moves with the uniform velocity U in X-direction.

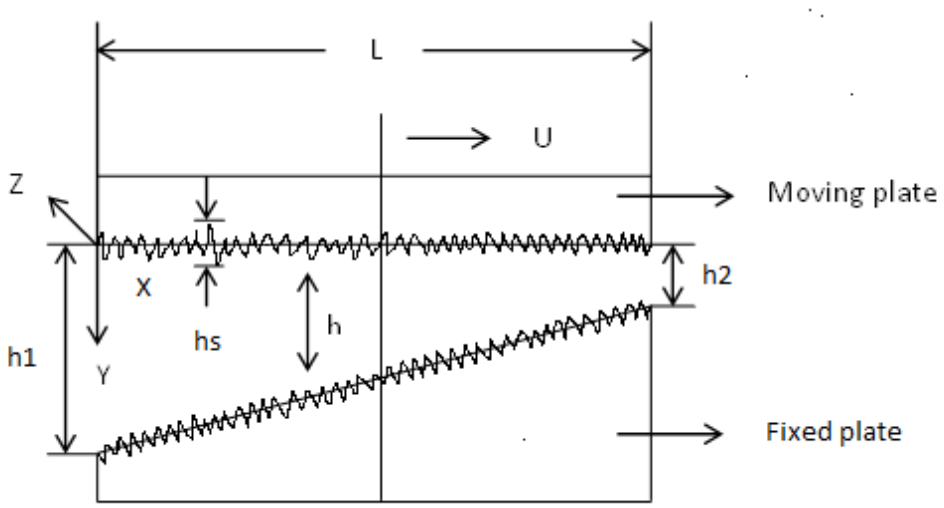

Figure 1: Configuration of bearing system

The bearing surfaces are assumed to be transversely rough. The thickness $h(x)$ of the lubricant film is given by

$$h(x) = \bar{h}(x) + h_s \tag{1}$$

Where $\bar{h}(x)$ is the mean film thickness and h_s is the deviation from the mean film thickness characterizing the random roughness of the bearing surfaces and h_s is considered to be stochastic in nature and governed by probability density function $f(h_s)$, $-c \leq h \leq c$, where c is the maximum deviation from mean film thickness. The mean α, the standard deviation σ and the measure of symmetry ε of the random variable h_s are defined by the relationship :

$$\alpha = E(h_s) \tag{2}$$

$$\sigma^2 = E[(h_s - \alpha)] \tag{3}$$

$$\varepsilon = E[(h_s - \alpha)^3] \tag{4}$$

It is easily observed that α, σ and ε are independent of x.

Where E is the expected value defined as

$$E(R) = \int_{-c}^{c} f(h_s) dh_s \quad (5)$$

While the probability density function is represented as

$$f(h_s) = \frac{35}{32c^7}(C^2 - h^2)^3, -C \le h \le C$$

$$= 0 \text{ , elsewhere} \quad (6)$$

The lubricant film is considered to be isoviscous and incompressible and the flow is laminar. The magnetic field is oblique to the stator as in Agrawal [1986]. Following discussions carried out by Bhat [2003] and Prajapati [1995] about the effect of various forms of magnitude of magnetic field is represented by

$$M^2 = Kx(L - x) \quad (7)$$

Where K is a suitably chosen constant from dimensionless point of view (Bhat and Deheri [1995]) and L is the length of bearing.

On the basis of assumptions, the equation governing the pressure distribution in the lubricant film satisfies a modified form of Reynolds' equation is given by

$$\frac{d}{dx}\left(p - \frac{\mu_0 \bar{\mu} M^2}{2}\right) = 6\mu U \left(\frac{h - \lambda h_2}{g(h)}\right) \quad (8)$$

Where $m = \frac{h_1 - h_2}{h_2}$

$h = h_2\left\{1 + m\left(1 - \frac{x}{L}\right)\right\}$

$g(h) = h^3 + 3h^2\alpha + 3h(\alpha^2 + \sigma^2) + (\alpha^3 + 3\sigma^2\alpha + \varepsilon)$

While μ_0 is the magnetic susceptibility, $\bar{\mu}$ is the free space permeability and μ is the lubricant viscosity

Integrating Eq. (8) w.r.t. x

$$p - \frac{\mu_0 \bar{\mu} M^2}{2} = 6\mu u \int_0^x \frac{h - \lambda h_2}{g(h)} dx \quad (9)$$

Introducing the dimensionless quantities in Eq. (9)

$\bar{\alpha} = \frac{\alpha}{h_2}$, $\bar{\sigma} = \frac{\sigma}{h_2}$, $\bar{\varepsilon} = \frac{\varepsilon}{h_2}$, $\mu^* = \frac{h_2^3 K \mu_0 \bar{\mu}}{\mu U}$, $P = \frac{h_2^3}{\mu U B^2} p$, $X = \frac{x}{L}$, $\overline{h_2} = \frac{h_2}{L}$

By Eq. (9),

The Pressure distribution in dimensionless form

$$P = \frac{\mu^*}{2}(X - X^2) + 6\overline{h_2}\int_0^X \frac{H-\lambda}{G(H)}dX \tag{10}$$

Where $H = 1 + m(1 - X)$

$G(H) = H^3 + 3H^2\bar{\alpha} + 3H(\bar{\alpha}^2 + \bar{\sigma}^2) + (\bar{\alpha}^3 + 3\bar{\sigma}^2\bar{\alpha} + \bar{\varepsilon})$

The associated boundary condition

$$P = 0 \text{ at } X = 0 \, and \, X = 1$$

By Eq. (10), we get,

$$\frac{\mu^*}{2}(X - X^2) + 6\overline{h_2}\int_0^X \frac{H-\lambda}{G(H)}dX = 0$$

$$\Rightarrow \lambda = \frac{\int_0^1 \frac{H}{G(H)}dx}{\int_0^1 \frac{1}{G(H)}dx}, \text{ Where } \lambda > 1 \tag{11}$$

Where $G(H) = H^3 + 3H^2\bar{\alpha} + 3H(\bar{\alpha}^2 + \bar{\sigma}^2) + (\bar{\alpha}^3 + 3\bar{\sigma}^2\bar{\alpha} + \bar{\varepsilon})$

and $H = 1 + m(1 - X)$

The load carrying capacity can be expressed in dimensionless form as

$$W = \int_0^1 P \, dX$$

$$= \int_0^1 \left(\frac{\mu^*}{2}(X - X^2) + 6\overline{h_2}\int_0^X \frac{H-\lambda}{G(H)}dX\right)dX$$

$$W = \frac{\mu^*}{12} + 6\overline{h_2}\int_0^1 \left[\int_0^X \frac{H-\lambda}{G(H)}dX\right] \tag{12}$$

3. Results and Discussions:

It is clearly observed that the dimensionless pressure distribution is presented by equation (10), while the profile of load carrying capacity in dimensional form is determined by equation (12). These performance characteristics depend on various parameters such as magnetization parameter μ*, length ratio h_2/L, aspect ratio m, roughness parameters σ, α and Ɛ etc.

Figure (2) dealing with the variation of load carrying capacity with respect to μ^* for various values of h_2/L suggest as the load carrying capacity increases sharply due to the magnetic fluid lubricant.

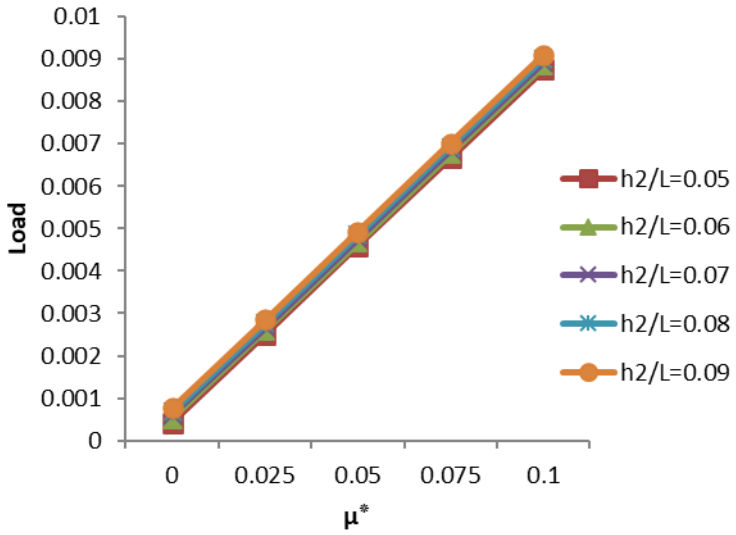

Figure 2: Variation of load carrying capacity with respect to μ* and h_2/L

Figures (3) - (5) shows the effect of h_2/L on dimensionless load carrying capacity for various values of α/h_2, ε/h_2 and m respectively. From these figures it is shown that the load carrying capacity increases considerably due to h_2/L. However, m has a positive effect in the sense that the load carrying capacity increase with increasing value of m.

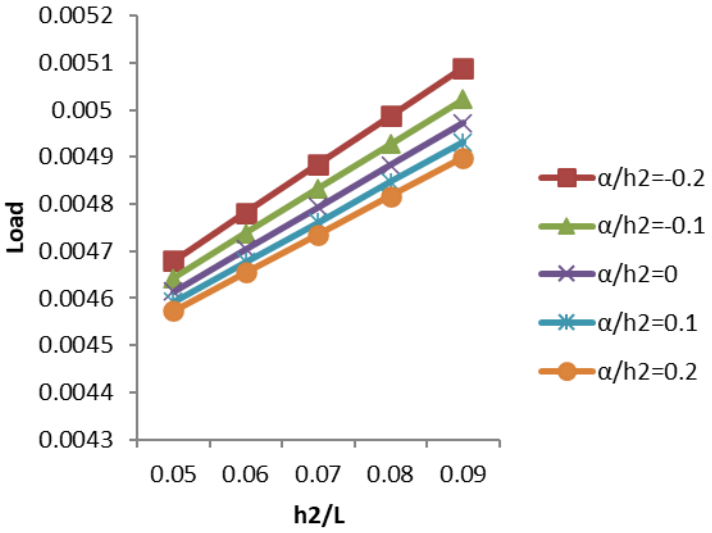

Figure 3: Variation of load carrying capacity with respect to h_2/L and α/h_2

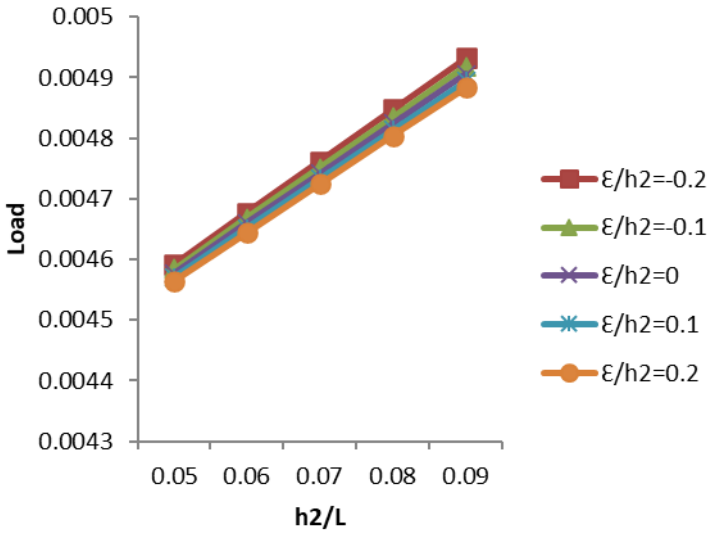

Figure 4: Variation of load carrying capacity with respect to h_2/L and ε/h_2

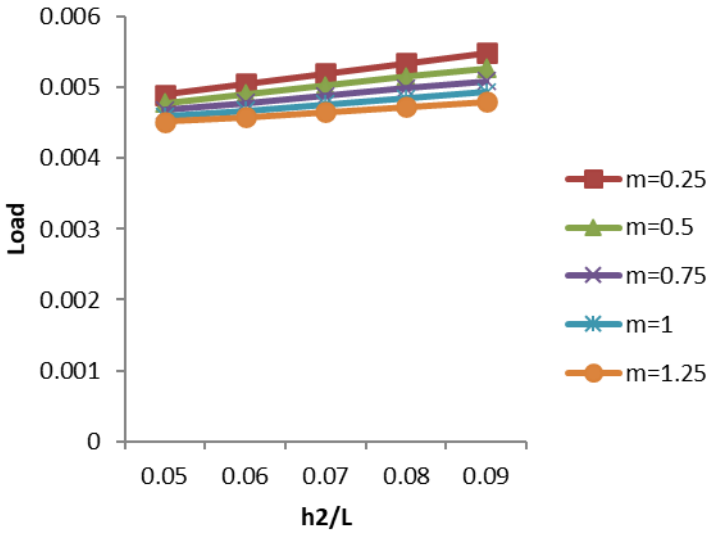

Figure 5: Variation of load carrying capacity with respect to h_2/L and m

Figure (6) represents the variation of load carrying capacity with respect to σ/h_2 for various values of α/h_2. From this figure it is clear that the load carrying capacity decreases due to σ/h_2 .

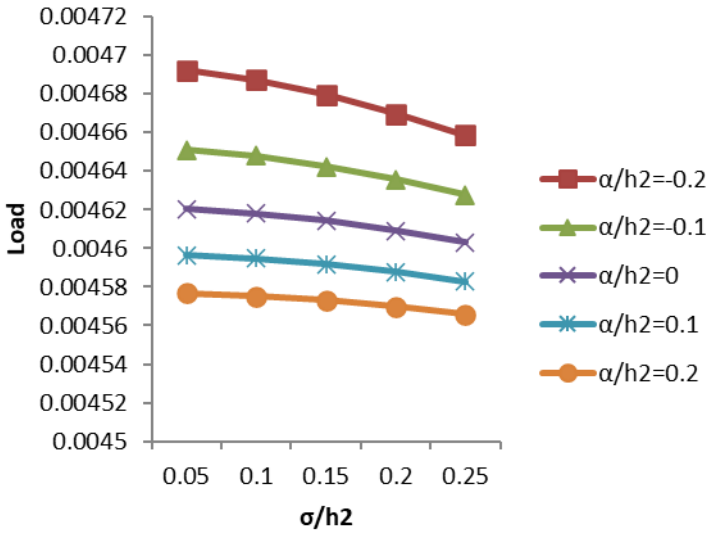

Figure 6: Variation of load carrying capacity with respect to σ/h_2 and α/h_2

Figures (7) shows the variation of load carrying capacity with respect to σ/h_2 for various values of m. From this figure it is clear that the load carrying capacity decreases slightly due to σ/h_2

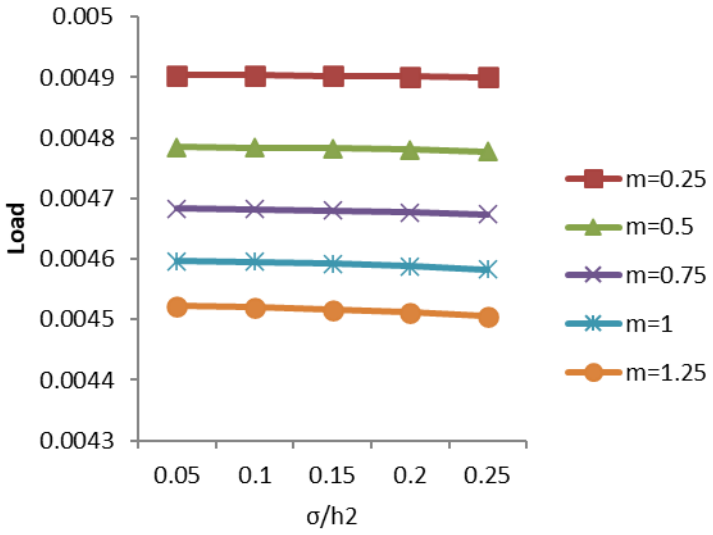

Figure 7: Variation of load carrying capacity with respect to σ/h_2 and m

Figures (8) represents that the variation of load carrying capacity with respect to α/h_2 for various values of $\mathcal{E}/h_2$. It is clearly seen that the load carrying capacity decreases marginally due to α/h_2.

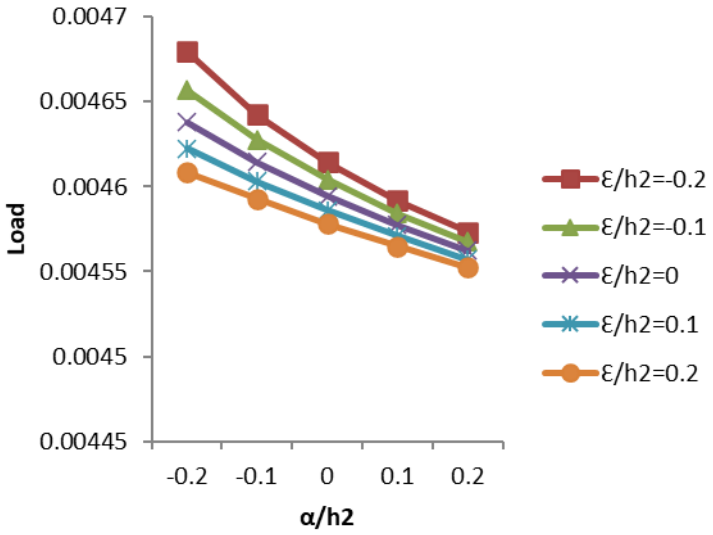

Figure 8: Variation of load carrying capacity with respect to α/h_2 and ε/h_2

Figure (9) presents the variation of load carrying capacity with respect to ε/h_2 for various values of m suggest as the load carrying capacity decreases marginally for increasing value of ε/h_2.

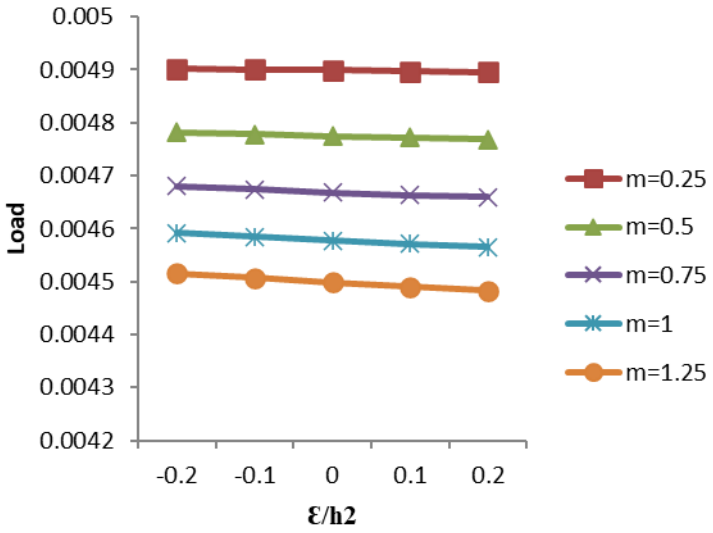

Figure 9: Variation of load carrying capacity with respect to ε/h_2 and m

Figures (10) & (11) show the variation of load carrying capacity with respect to m for various values of α/h_2, and h_2/L respectively. From this figures it is clear that the load carrying capacity decrease due to m.

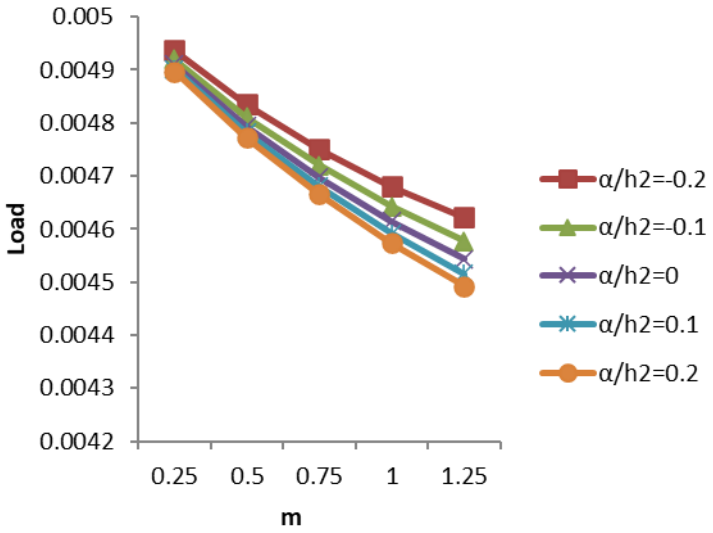

Figure 10: Variation of load carrying capacity with respect to m and α/h_2

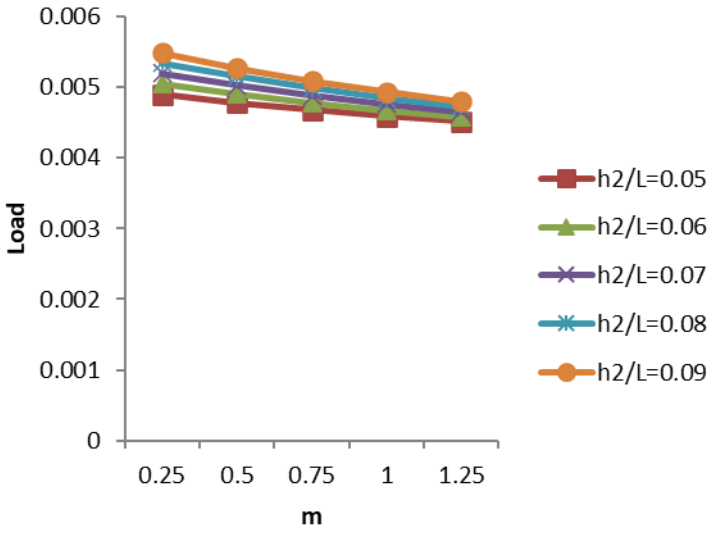

Figure 11: Variation of load carrying capacity with respect to m and h_2/L

4. Conclusion:

This investigation establishes that the performance of the bearing system can be improved considerably by choosing appropriate values of the aspect ratio and the outlet thickness ratio, in spite of the fact that the standard deviation has a negative effect on the performance of the bearing system. The analysis clearly demonstrates that magnetic fluid lubrication significantly enhances the load-carrying capacity and overall efficiency of the rough hyperbolic slider bearing. Although surface roughness introduces adverse effects, the negative influence can be effectively minimized through proper optimization of geometric parameters.

The study further highlights the crucial role of design parameters in governing hydrodynamic performance. By selecting suitable aspect ratios and outlet film thickness ratios, the bearing can maintain improved pressure generation and film stability, even under conditions of increased

surface irregularities. These findings underline the strong potential of magnetic fluids as advanced lubricants for enhancing bearing performance.
Overall, this work contributes valuable insights toward the design and optimization of magnetic-fluid-based bearing systems. Future research may focus on thermal effects, dynamic loading, non-Newtonian magnetic fluids, and experimental validation to broaden the applicability of the present model.

References:

1. Purday, H. (1947). *Steam line flow*. Constable.
2. Pinkus, O., & Stemlitch, B. (1961). *Theory of hydrodynamic lubrication*. McGraw-Hill.
3. Cameron, A. (1972). *Basic theory of lubrication*. Ellis Harwood; Halsted Press; John Wiley & Sons.
4. Prakash, J., & Vij, S. K. (1973). Hydrodynamic lubrication of a porous slider. *Journal of Mechanical Engineering Science, 15*, 222–234.
5. Bhat, M. V., & Patel, C. M. (1981). The squeeze film in an inclined porous slider bearing. *Wear, 66*, 189–193.
6. Bagci, C., & Singh, A. P. (1983). Hydrodynamic lubrication of a finite slider bearing: Effect of one-dimensional film shape and computer-aided optimum designs. *ASLE Transactions: Journal of Lubrication Technology, 105*, 48–66.
7. Ajwaliya, M. B. (1984). *Hydrodynamic lubrication of a secant shaped porous slider* (Master's thesis). S. P. University, India.
8. Hamrock, B. J. (1994). *Fundamentals of fluid film lubrication*. McGraw-Hill.
9. Mitchell, J. (1950). *Lubrication: Its principle and practice*. Blackie.
10. Davis, M. G. (1963). The generation of pressure between rough fluid-lubricated moving deformable surfaces. *Lubrication Engineering, 19*, 246.
11. Burton, R. A. (1963). Effect of two-dimensional sinusoidal roughness on the load-support characteristics of a lubricant film. *Journal of Basic Engineering, ASME, 85*, 258–264.
12. Tzeng, S. T., & Saibel, E. (1967). Surface roughness effect on slider bearing lubrication. *Journal of Lubrication Technology, ASME, 10*, 334–338.
13. Christensen, H., & Tonder, K. C. (1969a). Tribology of rough surfaces: Stochastic models of hydrodynamic lubrication. *Tribology International, 10*, 69–78.
14. Christensen, H., & Tonder, K. C. (1969b). Tribology of rough surfaces: Parametric study and comparison of lubrication models. *Tribology International, 22*, 69–78.
15. Christensen, H., & Tonder, K. C. (1970). The hydrodynamic lubrication of rough bearing surfaces of finite width. *ASME-ASLE Lubrication Conference*, Cincinnati, Ohio, Paper No. 70-Lub-7.
16. Tonder, K. C. (1972). Surface distributed waviness and roughness. In *Proceedings of the First World Conference in Industrial Tribology* (Vol. 3A, pp. 01–08). New Delhi, India.
17. Berthe, D., & Godet, M. (1973). A more general form of Reynolds equation: Application to rough surfaces. *Wear, 27*, 345–357.
18. Ting, L. L. (1975). Engagement behavior of lubricated porous annular disks: Part I—Squeeze film phase, surface roughness, and elastic deformation effects. *Wear, 34*, 159–182.

19. Prakash, J., & Tiwari, K. (1982). Lubrication of porous bearings with surface corrugations. *Journal of Lubrication Technology, ASME, 104*, 127–134.
20. Prakash, J., & Tiwari, K. (1983). Roughness effect in porous circular squeeze plates with arbitrary wall thickness. *Journal of Lubrication Technology, ASME, 105*, 90–95.
21. Prajapati, B. L. (1991). Behaviour of squeeze film between rotating porous circular plates: Surface roughness and elastic deformation effects. *Pure and Applied Mathematical Sciences, 33*, 27–36.
22. Prajapati, B. L. (1992). Squeeze behaviour between rotating porous circular plates with a concentric circular pocket: Surface roughness and elastic deformation effects. *Wear, 152*, 301–307.
23. Guha, S. K. (1993). Analysis of dynamic characteristics of hydrodynamic journal bearing with isotropic roughness effects. *Wear, 167*, 173–179.
24. Gupta, J. L., & Deheri, G. M. (1996). Effects of roughness on the behaviour of squeeze film in a spherical bearing. *Tribology Transactions, 39*, 99–102.
25. Andharia, P. I., Gupta, J. L., & Deheri, G. M. (1997). Effects of longitudinal surface roughness on hydrodynamic lubrication of slider bearings. In *Proceedings of the Tenth International Conference on Surface Modification Technologies* (pp. 872–880). Institute of Materials, London.
26. Andharia, P. I., Gupta, J. L., & Deheri, G. M. (1999). Effects of transverse surface roughness on the behavior of squeeze film in a spherical bearing. *Journal of Applied Mechanics and Engineering, 4*, 19–24.
27. Verma, R. C. (1986). Magnetic fluid-based squeeze film. *International Journal of Engineering Science, 24*, 395–401.
28. Agrawal, V. K. (1986). Magnetic fluid-based porous inclined slider bearing. *Wear, 107*, 133–139.
29. Bhat, M. V., & Deheri, G. M. (1991). Squeeze film behaviour in porous annular discs lubricated with magnetic fluid. *Wear, 151*, 123–128.
30. Bhat, M. V., & Deheri, G. M. (1991). Porous composite slider bearing lubricated with magnetic fluid. *Japanese Journal of Applied Physics, 30*, 2513–2514.
31. Bhat, M. V., & Deheri, G. M. (1995). Porous slider bearing with squeeze film formed by a magnetic fluid. *Pure and Applied Mathematical Sciences, 39*, 39–43.
32. Bhat, M. V. (2003). *Lubrication with a magnetic fluid*. Team Spirit (India) Pvt. Ltd.
33. Shah, R. C., & Bhat, M. V. (2003). Effect of slip velocity in a porous secant-shaped slider bearing with a ferrofluid lubricant. *Fizika A, 12*, 1–8.
34. Deheri, G. M., Andharia, P. I., & Patel, R. M. (2005). Transversely rough slider bearing with squeeze film formed by a magnetic fluid. *International Journal of Applied Mechanics and Engineering, 10*, 53–76.